

Planar sensor properties of perovskite $\text{Sr}(\text{Ti}_{1-x}\text{Fe}_x)\text{O}_{3-\delta}$ powders prepared by a sol-gel method

Woonyoung Lee^a, Dongmyung Na^b and Jinseong Park^{c,*}

^aThe Research Institute of Advanced Engineering Tech. Chosun University, Gwangju, 501-759 Korea

^bGaustek Co., Gwangju, 500-480, Korea

^cDept. of Advanced Materials and Eng., Chosun University, Gwangju, 501-759, Korea

An oxygen sensor for an automobile exhaust system was integrated by planar technology. Powders of perovskite $\text{SrTi}_{1-x}\text{Fe}_x\text{O}_{3-\delta}$ were synthesized by a sol-gel method. Micro-powders to compare the properties of powders were also prepared by a solid state reaction after mixing of commercial reagents of SrCO_3 , TiO_2 , and Fe_2O_3 . A paste based on nano- and micro-powders was prepared to make a planar device on an Al_2O_3 substrate by silk screen printing technology. The phase formation and microstructure were analyzed by XRD and SEM, respectively. O_2 sensing and electrical properties were measured as a function of thermal treatment conditions, atmosphere, time and temperature. The precursor was transformed into $\text{SrTi}_{1-x}\text{Fe}_x\text{O}_{3-\delta}$ at 800~1100 °C in ambient atmosphere. Zero TCR(temperature coefficient of resistance) for perovskite $\text{SrTi}_{1-x}\text{Fe}_x\text{O}_{3-\delta}$ powders was measured over 600 °C. There were no interference effect to CH_4 , CO , NO_2 and CO_2 , but an excellent response and recovery characteristics with oxygen concentration.

Key words: $\text{SrTi}_{1-x}\text{Fe}_x\text{O}_{3-\delta}$, Perovskite structure, Sol-gel precipitation, Oxygen sensor.

Introduction

There has been a lot of demand for the detection and control of air pollution arising from various fields such as industry, automobiles, etc., which cause adverse effects on a global environment. Semiconducting type gas sensors compared to solid electrolyte sensors such as, the ZrO_2 sensor are also focusing to detect various pollutants of the atmosphere such as CO , NO_x and SO_x [1-2]. The drawback of semiconducting sensors is the temperature dependence of conductivity:

$$\sigma(P_{\text{O}_2}, T) \propto P_{\text{O}_2}^{1/4} \exp\left(-\frac{E_a}{kT}\right) \quad (1)$$

It has been reported that semiconducting oxides such as perovskite Fe-doped SrTiO_3 [3-4] show a zero temperature coefficient of resistance (zero-TCR) [5-6].

The electrical property can be changed by a dopant, an oxygen excess or deficit in these perovskite oxides, too.

Thus, researchers have examined perovskite $\text{SrTi}_{1-x}\text{Fe}_x\text{O}_{3-\delta}$ with semiconducting behaviors to use as alternatives to a ZrO_2 oxygen sensor due to its zero-TCR and its ease of fabrication.

The $\text{SrTi}_{1-x}\text{Fe}_x\text{O}_{3-\delta}$ sensors using commercial powders reported that the grain size was large and the temperature for a manufacturing operation requires high temperature treatments, for example calcination about 1100 °C and

sintering about 1200 °C.

In this study, the article suggests the low temperature process to make the materials of zero-TCR $\text{SrTi}_{1-x}\text{Fe}_x\text{O}_{3-\delta}$ by nano-particles technology, with a sol-gel method. The possibility for automobile oxygen sensors was also investigated through the characterization of the electric properties, microstructures and gas sensitivity.

Experimental

$\text{SrTi}_{1-x}\text{Fe}_x\text{O}_{3-\delta}$ nano-particles with a perovskite structure were synthesized by a sol-gel reaction. The starting chemicals are strontium nitrite, titanium butoxide, iron nitride nona hydrate as precursors. The gel was calcined at 800 ~ 1100 °C for 6 hours. The planar device of a 2 × 3 mm chip size was fabricated on an alumina substrate by thick film technology. The paste for thick film printing used the nano-particles prepared by the sol-gel method. The sensor was sintered at 900 ~ 1100 °C for 1 hour after printing on an alumina substrate. Pt pastes and wires were used as electrodes to measure the electrical properties. An X-ray diffractometer (XRD) and scanning electron microscope (SEM) were used to observe the phase formation and microstructure, respectively. Sensing properties were measured from 450 °C to 900 °C as a function of the concentration of O_2 , CH_4 , CO , CO_2 and NO_2 .

Results and discussion

Fig. 1 shows XRD patterns of $\text{SrTi}_{0.5}\text{Fe}_{0.5}\text{O}_{3-\delta}$ powder at various calcination temperatures. Gel powders manufactured

*Corresponding author:
Tel : +82-62-230-7193
Fax: +82-62-222-5116
E-mail: jsepark@chosun.ac.kr

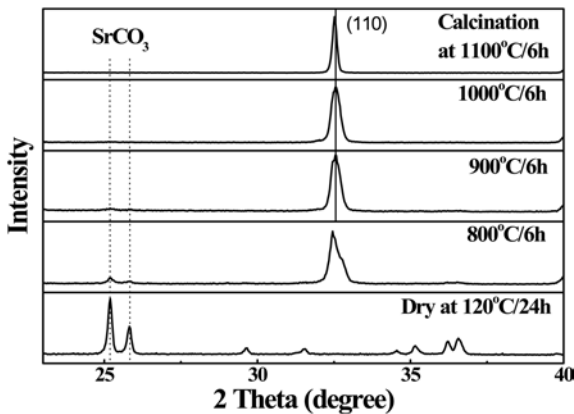


Fig. 1. XRD data of $\text{SrTi}_{0.5}\text{Fe}_{0.5}\text{O}_{3-\delta}$ powder at a series of calcination temperatures.

with the sol-gel method exists with SrCO_3 , TiO_2 and Fe hydroxides after being dried at 120°C for 24 hours. Even though perovskite structures were formed after heat treatment above 800°C temperature, a very small amount of unreacted SrCO_3 remained until 800°C . SrCO_3 completely disappeared after calcination at 900°C and the single perovskite structure was formed. At a high calcination temperature the half width came to be narrow. The 2θ value of its (1 1 0) peak was 32.575° , 32.545° , 32.515° , and the lattice parameters were calculated to be 3.884 \AA , 3.887 \AA , 3.891 \AA after sintering at 900°C , 1000°C and 1100°C , respectively. An increase of the lattice parameters means a weakening of the binding force.

Fig. 2 shows grain size of calcined powder at 800°C (a), and devices sintered at (b) 900°C for 1 h, (c) 1000°C for 1 h and (d) 1100°C for 1 h after calcinations

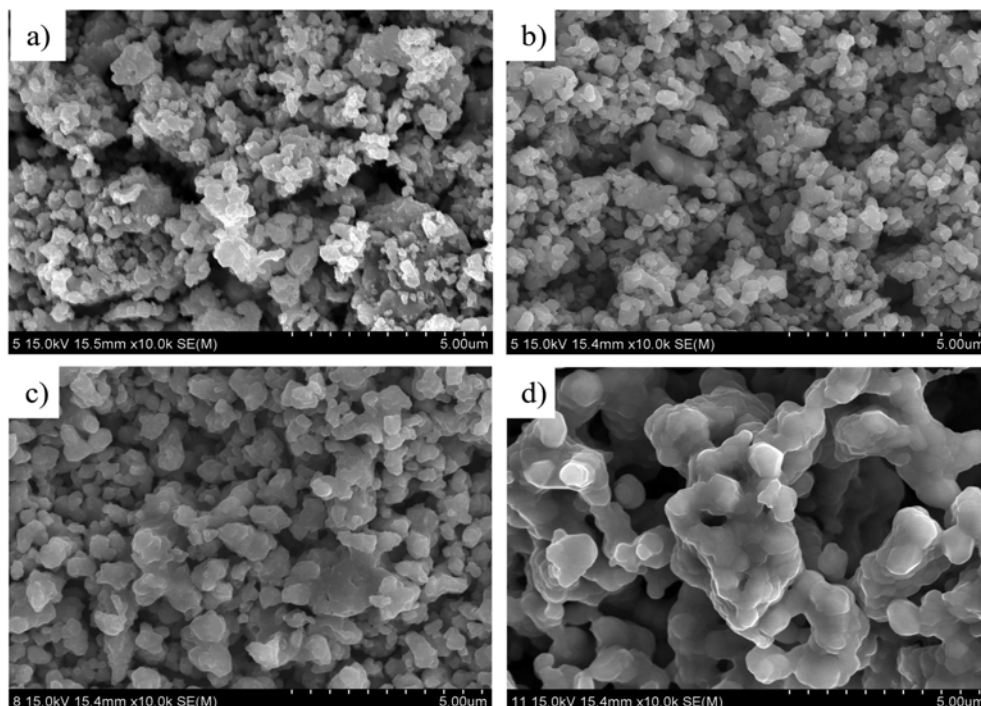


Fig. 2. Grain size variation of $\text{SrTi}_{0.5}\text{Fe}_{0.5}\text{O}_{3-\delta}$ films on Al_2O_3 substrates as a function of sintering temperature.

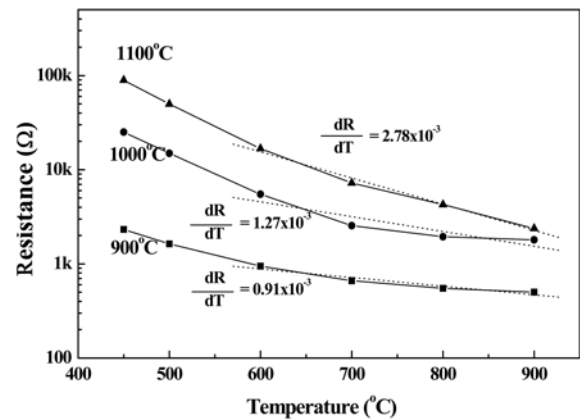


Fig. 3. Resistance behavior with measurement temperature for the sintered thick films.

at 800°C for 6 hours, respectively. The particle size was about 100 nm after calcinations at 800°C . The particle size was increased to $0.5 \mu\text{m}$ and $1.0 \mu\text{m}$ after sintering at 900°C and 1000°C respectively. A network structure, connected continuously by $3.0 \mu\text{m}$ particles, was observed after sintering at 1100°C in Fig. 2(d).

As a result, it was thought that perovskite-structured $\text{SrTi}_{0.5}\text{Fe}_{0.5}\text{O}_{3-\delta}$, sintered at 900°C and 1100°C , was suitable as a sensing material for gas sensors because of the near spherical shape and sub-micrometer particle size.

Fig. 3 shows the resistance behavior with measurement temperature of $\text{SrTi}_{0.5}\text{Fe}_{0.5}\text{O}_{3-\delta}$, sensor sintered at 900°C ~ 1100°C for 1 hour in an air atmosphere. The resistance of $\text{SrTi}_{0.5}\text{Fe}_{0.5}\text{O}_{3-\delta}$ sensors increased with the sintering temperature. $\text{SrTi}_{0.5}\text{Fe}_{0.5}\text{O}_{3-\delta}$ was stable stoichiometrically at $3-\delta$ value of 2.75. The 2θ of (110) peak was 32.262° (JCPDS card #841003) and the

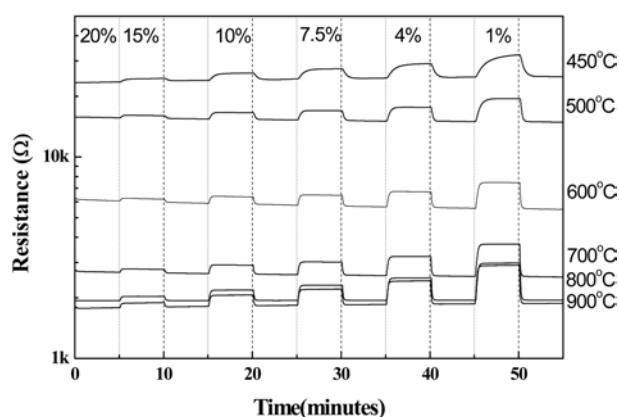
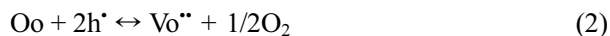


Fig. 4. Resistance behavior with oxygen concentration as a function of measurement temperature for $\text{SrTi}_{0.5}\text{Fe}_{0.5}\text{O}_{3-\delta}$ thick films on Al_2O_3 .

lattice parameter was 3.909 Å at a 3- δ value of 2.75.

From the XRD patterns of the (110) peak with sintering temperature in Fig. 1, the lattice parameters were 3.884 Å, 3.887 Å and 3.891 Å at 900 °C, 1000 °C and 1100 °C, respectively. It was found that the lattice parameter was close to 3.909 Å with the sintering temperature. This can be explained from a decrease of the oxygen concentration within the lattice and covalent bonding strength with the sintering temperature.

The resistance increases due to a decrease of the hole concentration according to equation 1.



A semiconducting property was observed in the case of the $\text{SrTi}_{0.5}\text{Fe}_{0.5}\text{O}_{3-\delta}$ sensor sintered at 1100 °C. So, the resistance was decreased successively as the measuring temperature was increased. On the other hand, the measuring temperature range in which resistance hardly varied, namely TCR (Temperature Coefficient of Resistance) was zero, existed above 600 °C in the case of sintering of 900 °C. This is a rare phenomenon, considering that a variation of oxygen concentration within the lattice is found in ceramics above 500 °C. From this result, it is expected that $\text{SrTi}_{0.5}\text{Fe}_{0.5}\text{O}_{3-\delta}$ can be a candidate for oxygen sensors because its resistance can be varied by the oxygen concentration irrespective of the operating temperature. The TCR characteristics of $\text{SrTi}_{0.5}\text{Fe}_{0.5}\text{O}_{3-\delta}$ could result from the compensation of the increased hole concentration with the measuring temperature by the increased oxygen concentration within the lattice. This could also be related with the diffusion length of oxygen atoms with the particle size or sintering temperature. Oxygen atoms in lattices are difficult to remove due to the long diffusion length of oxygen atoms in a large particle size grown by sintering at a high temperature of 1100 °C. In the case of a low sintering temperature, the fast removal of oxygen atoms within a lattice due to a small particle size can compensate the decrease of resistance with increasing

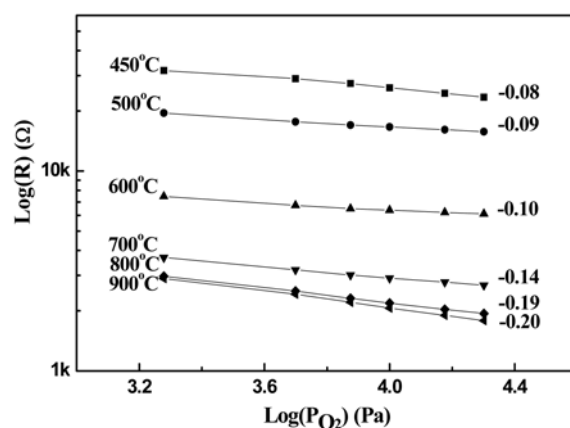


Fig. 5. Sensitivity behavior as a function of the measurement temperature for $\text{SrTi}_{0.5}\text{Fe}_{0.5}\text{O}_{3-\delta}$ sensor sintered at 900 °C.

measurement temperature.

Fig. 4 shows the electric resistance with oxygen concentration as a function of the measurement temperature for $\text{SrTi}_{0.5}\text{Fe}_{0.5}\text{O}_{3-\delta}$ samples heated at 900 °C for 1 hour. The response and recovery properties were measured from the initial state of a 20% oxygen content. $\text{SrTi}_{0.5}\text{Fe}_{0.5}\text{O}_{3-\delta}$ powder showed excellent properties, a fast response and reproducibility on oxygen gas at operating temperatures above 450 °C.

It has been reported that the operating temperature of oxygen sensors fabricated from a solid solution had a similar trend with those fabricated by the sol-gel method above 700 °C. Oxygen sensors fabricated by the sol-gel method can have the possibility of a lowering operating temperature and sintering temperature of about 100 ~ 200 °C.

Fig. 5 shows the sensitivity behavior with the measurement temperature for a $\text{SrTi}_{0.5}\text{Fe}_{0.5}\text{O}_{3-\delta}$ sensor. Their sensitivity with increasing measurement temperature at 450 ~ 900 °C was observed to be close to the theoretical value ($m = 1/6 \sim 1/4$) [7].

Fig. 6. Interference effects on CH_4 , CO, NO_2 and CO_2 during constant 20 vol% oxygen flow for $\text{SrTi}_{0.5}\text{Fe}_{0.5}\text{O}_{3-\delta}$ at 700 °C.

It is necessary that the interference effect of other gases besides oxygen gas was investigated for effective application as oxygen gas sensors. Fig. 6 shows the resistance variation of our sensor devices by gases generated during combustion such as, CH_4 , CO, NO_2 and CO_2 . It was found out that resistance variation by other gases besides oxygen was insignificant and our sensor devices had excellent selectivity to oxygen.

Conclusions

The sensitivity of $\text{Ti}_{0.5}\text{Fe}_{0.5}\text{O}_{3-\delta}$ powders, prepared by a sol-gel method, to oxygen gas was characterized in this study. $\text{Ti}_{0.5}\text{Fe}_{0.5}\text{O}_{3-\delta}$ powders had perovskite phases with a cubic structure and their powder size was 100 nm after the calcination above 800 °C. Their grain

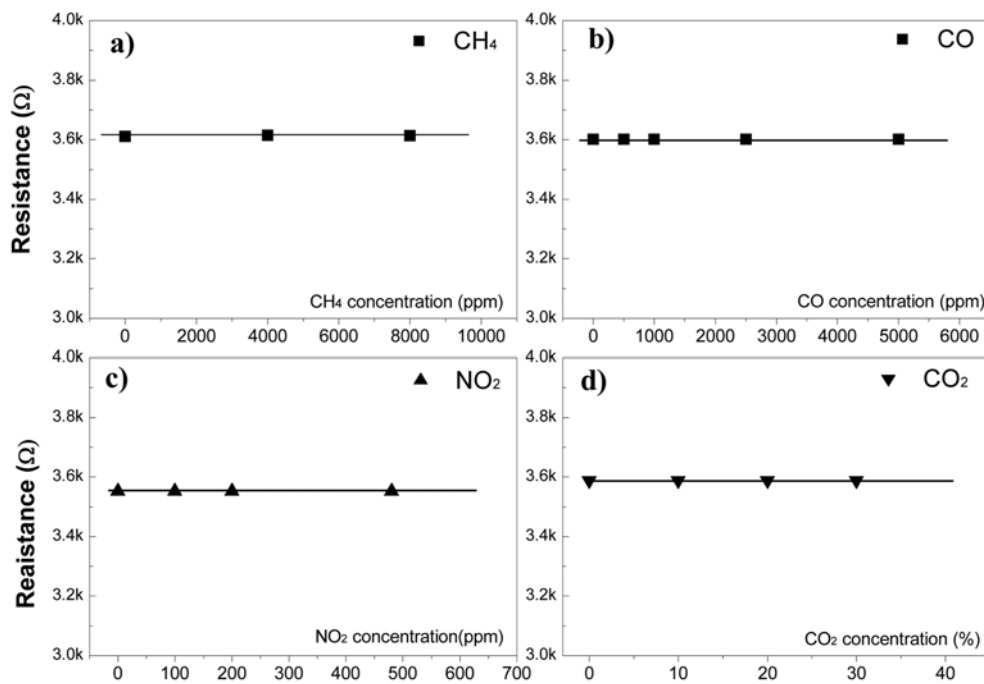


Fig. 6. Interference effects of CH₄, CO, NO₂ and CO₂ during a constant 20 vol% oxygen flow for SrTi_{0.5}Fe_{0.5}O_{3-δ} at 700 °C.

size increased and electrical conductivity decreased with the sintering temperature. The response of a Ti_{0.5}Fe_{0.5}O_{3-δ} device began from 450 °C and their sensitivity was improved above 700 °C. Their sensitivity at 900 °C was observed to be close to theoretical with a value of -0.2. The response time of a Ti_{0.5}Fe_{0.5}O_{3-δ} sensor to oxygen gas was less than 1 second.

It was found out that the samples of Ti_{0.5}Fe_{0.5}O_{3-δ} sensor almost never react with CH₄, CO, CO₂, and NO₂, only oxygen.

Acknowledgements

This Research was supported by Basic Science Research program through the National Research Foundation of Korea (NRF) funded by the Ministry of

Educational, Science and Technology (2012-0002040).

References

1. M.Z. Atashbar, H.T. Sun, B. Gong, W. Wlodarski and T. Lamb, *Thin Solid Films* 326 (1998) 238-244.
2. G.P. Choi, G.H. Jin, S.H. Park, W.Y. Lee, J.S. Park, *Journal of nanoscience and nanotechnology* 7 (2007) 3481-3846.
3. K. Szner, M. Kaspar and R. Moos, *Sens. Actuators B* 139 (2009) 394-399.
4. A. Rothschild, S.J. Litzelman, H.L. Tuller, W. Menesklou, T. Schneider and E.I. Tiffée, *Sens. Actuators B* 108 (2005) 223-230.
5. G. Neri, A. Bonavita, G. Micali, G. Rizzo, R. Licheri, R. Orru and G. Cao, *Sens. Actuators B* 126 (2007) 258-265.
6. S.J. Litzelman, A. Rothschild and H.L. Tuller, *Sens. Actuators B* 108 (2005) 231-237.
7. J.W. Fergus, *Sens. Actuators B* 123 (2007) 1169-1179.